Reflection-mode continuous-wave 0.15λ-resolution terahertz solid immersion microscopy of soft biological tissues

N. V. Chernomyrdin, A. S. Kucheryavenko, G. S. Kolontaeva, G. M. Katyba, I. N. Dolganova, P. A. Karalkin, D. S. Ponomarev, V. N. Kurlov, I. V. Reshetov, M. Skorobogatiy, V. V. Tuchin, and K. I. Zaytsev

Citation: Appl. Phys. Lett. **113**, 111102 (2018); doi: 10.1063/1.5045480
View online: https://doi.org/10.1063/1.5045480
View Table of Contents: http://aip.scitation.org/toc/apl/113/11
Published by the American Institute of Physics

Reflection-mode continuous-wave 0.15λ-resolution terahertz solid immersion microscopy of soft biological tissues

N. V. Chernomyrdin,[1,2,3] A. S. Kucheryavenko,[3] G. S. Kolontaeva,[3] G. M. Katyba,[3,4] I. N. Dolganova,[2,3,4] P. A. Karalkin,[5,6] D. S. Ponomarev,[7] V. N. Kurlov,[2,4] I. V. Reshetov,[2] M. Skorobogatiy,[8] V. V. Tuchin,[9,10,11] and K. I. Zaytsev[1,2,3,a)]

[1]*Prokhorov General Physics Institute of the Russian Academy of Sciences, Moscow 119991, Russia*
[2]*Sechenov First Moscow State Medical University, Moscow 119991, Russia*
[3]*Bauman Moscow State Technical University, Moscow 105005, Russia*
[4]*Institute of Solid State Physics of the Russian Academy of Sciences, Chernogolovka 142432, Russia*
[5]*3D Bioprinting Solutions, Moscow 115409, Russia*
[6]*National Medical Research Center of Radiology, Moscow 125284, Russia*
[7]*Institute of Ultra-High Frequency Semiconductor Electronics of the Russian Academy of Sciences, Moscow 117105, Russia*
[8]*Department of Engineering Physics, Polytechnique Montreal, Montreal, Quebec H3T 1J4, Canada*
[9]*Saratov State University, Saratov 410012, Russia*
[10]*Tomsk State University, Tomsk 634050, Russia*
[11]*Institute of Precision Mechanics and Control of the Russian Academy of Sciences, Saratov 410028, Russia*

(Received 20 June 2018; accepted 27 August 2018; published online 10 September 2018)

We have developed a method of terahertz (THz) solid immersion (SI) microscopy for continuous-wave reflection-mode imaging of soft biological tissues with a sub-wavelength spatial resolution. In order to achieve strong reduction in the dimensions of the THz beam caustic, an electromagnetic wave is focused into the evanescent field volume behind a medium with a high refractive index. We have experimentally demonstrated a 0.15λ-resolution of the proposed imaging modality at $\lambda = 500\,\mu$m, which is beyond the Abbe diffraction limit and represents a considerable improvement over the previously-reported arrangements of SI imaging setups. The proposed technique does not involve any sub-wavelength near-field probes and diaphragms, thus, avoiding the THz beam attenuation due to such elements. We have applied the developed method for THz imaging of various soft tissues: a plant leaf blade, cell spheroids, and tissues of the breast *ex vivo*. Our THz images clearly reveal sub-wavelength features in tissues, therefore, promising applications of THz SI microscopy in biology and medicine. *Published by AIP Publishing*. https://doi.org/10.1063/1.5045480

Over the past decades, many modalities of terahertz (THz) imaging have been vigorously explored.[1,2] Among various applications of THz imaging, considerable attention has been paid to its use in medical diagnosis,[3] where it yields a label-free differentiation between healthy tissues and malignancies in various localizations.[4–6] Most of the modern THz biomedical imaging systems rely on conventional lens- and mirror-based optics and possess a diffraction-limited spatial resolution.[7] Thus, even for a THz optical system with the largest-possible numerical aperture NA = 1.0, the Abbe diffraction limit sets the resolution to $\simeq 0.61\lambda$ (λ is a free-space wavelength of light).[8] Since the wavelength of THz radiation is on the order of hundreds of microns, the diffraction phenomena pose significant limitations on the accuracy of malignancy margin detection, thus, pushing further developments into the realm of sub-wavelength-resolution THz imaging.

Several approaches for high resolution THz imaging have been recently proposed. Among them, THz holography[9] and synthetic aperture imaging[10] yield slightly sub-wavelength spatial resolution, but require complicated computations for resolving the inverse ill-posed problems.[11] In turn, while the near-field THz imaging easily overcomes the diffraction limit and provides an impressive spatial resolution down to 10^{-2}–$10^{-3}\lambda$,[12–16] it normally employs detection of very weak signals scattered by sub-wavelength probes placed at the object plane. This requires powerful emitters and sensitive detectors, which are still rare, expensive, and cumbersome.

Other promising approaches for high-resolution THz imaging rely on the effects of electromagnetic field localization at the shadow side of a mesoscale dielectric particle,[17] where both the photonic jet effect[18] and the solid immersion (SI) phenomenon[19] can provide sub-wavelength focusing. Among these approaches, we would particularly note SI microscopy, which employs an electromagnetic wave focusing into the evanescent field volume behind a high refractive index material in order to achieve reduction in the dimensions of a focal spot. This technique was first introduced in the visible (VIS) and infrared (IR) ranges, and was applied in microscopy,[20] optical data storage,[20] Raman[21] and thermal[22] imaging, and testing of integrated electrical circuits.[23] Later, it was transferred to the millimeter-wave (MMW)[24] and THz[25] bands. Most recently, in Ref. 26, we proposed a structure of the THz SI lens, which is based on the favorable combination of a wide-aperture aspherical singlet and a hypohemispherical lens, and yields 0.35λ-resolution.

Among all of the above-mentioned approaches, the SI microscopy seems to be a promising tool for THz biophotonics thanks to a combination of sub-wavelength resolution

a)Author to whom correspondence should be addressed: kirzay@gmail.com

and high optical throughout, as no sub-wavelength probes are used. Unfortunately, none of the existing configurations of the THz SI lenses are suitable for solving the demanding problems in biology and medicine owing to the problem of soft tissue handling at the focal plane of the SI lens during point-by-point reflection-mode imaging. A straightforward approach, which involves direct contact between the high refractive index lens and the moving tissue, as reported in Ref. 25 could lead to distortions in the image due to inadvertent mechanical compression of the tissues and the occlusion effect. These image distortions are of crucial importance in THz bioimaging since the label-free differentiation between healthy and pathological tissues typically requires high measurement accuracy and image clarity.[3–6]

In order to mitigate a challenging problem posed by the sub-wavelength-resolution THz imaging of soft biological tissues, in this letter, we propose a method of THz SI microscopy, which allows handling of the tissue sample at the SI lens focal plane during continuous-wave (CW) reflection-mode imaging, while yielding an advanced spatial resolution. This configuration for the THz SI microscopy achieves a 0.15λ-resolution at $\lambda = 500\,\mu$m, which is superior compared to other existing SI lens configurations reported in the MMW, THz, IR, and VIS spectral ranges.[22–28] We then apply the developed THz SI microscopy setup to imaging of different soft tissues and cell structures: a plant leaf, cell spheroids, and tissues of the breast *ex vivo*. The acquired images reveal sub-wavelength features in tissues thus highlighting the potential of the proposed THz imaging modality for various demanding applications in biology and medicine.

In Fig. 1, the schematic of the proposed THz SI lens arrangement is presented. This SI lens is comprised of three optical elements: a wide-aperture aspherical singlet (made of high-density polyethylene—HDPE), a hypohemisphere, and a movable planar sample holder (both made of high resistivity float-zone silicon—HRFZ-Si). The aspherical singlet features a focal length of 15 mm and an entrance pupil diameter of 25 mm.[7] The hemisphere has a diameter of $D = 10$ mm and a thickness of $l = 4.7$ mm. The position of the hemisphere is adjusted so that the spherical wavefront of the focused THz beam is concentric with the lens' spherical surface. Additionally, by design, the lens flat terminating surface is parallel to its focal plane. The aspherical singlet and the hypohemisphere are rigidly fixed, while the sample holder is mounted on a motorized X–Y translation stage.

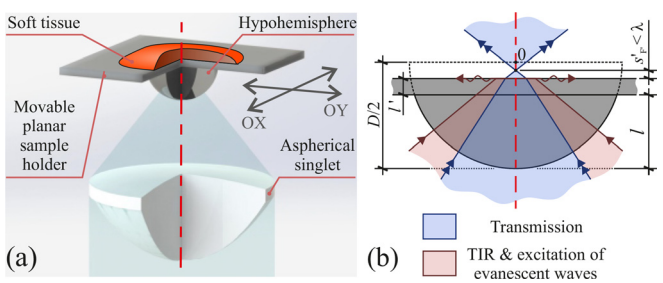

FIG. 1. THz SI lens for imaging of soft tissues: (a) schematic of a THz SI lens comprised of a wide-aperture aspherical singlet (made of HDPE), a rigidly-fixed hypohemisphere, and a movable planar sample holder (both made of HRFZ-Si); (b) schematic of beam focusing by a SI lens illustrating a contribution of transmitted beam and evanescent waves on the THz beam focusing; TIR stands for a total internal reflection.

The sample holder has a thickness of $l' = 0.25$ mm and completes the hypohemispherical lens to an almost perfect hemisphere ($l + l' = 4.95$ mm, while $D/2 = 5$ mm), which is a core optical element in SI lens that leads to sub-wavelength image resolution, while also serving as a sample holder for tissue samples. Furthermore, this approach of tissue handling prevents their shrinkage (or other mechanical perturbations), thus, eliminating distortions of THz images. Using a paraxial approximation, we can estimate a back focal distance of the resultant THz SI lens $s'_{F'} \simeq (D/2 - l - l')n_{obj}/n_{Si}$, where $n_{Si} = 3.415$ and n_{obj} stand for the THz refractive indicies of the HRFZ-Si and the object of interest. In the studied compound SI lens, no oil was used for the reduction of friction between the two movable elements. In fact, during our experiments, we did not observe any issues associated with either mechanical damage of the two sliding flat surfaces of the HRFZ-Si optical elements, or image distortion due to formation of air gaps between these surfaces. However, these effects are difficult to quantify at this time, and further investigations are in order.

Schematic of a SI microscope operating in the reflection mode is shown in Fig. 2. As a source of CW THz radiation at $\lambda = 500\,\mu$m, we use a backward-wave oscillator (BWO). As a detector of the THz beam intensity, we use a Golay cell. A 22-Hz-mechanical chopper is used to modulate the intensity of the THz beam since the Golay cell only detects the non-stationary electromagnetic wave intensity, while an attenuator is used to prevent the detector overload. To homogenize the intensity of a THz beam over its cross-section, a 1-mm-diameter metal diaphragm is used at the focal plane of a $1\times$-telescopic system, as shown in Fig. 2.

In order to find a spatial resolution of our THz SI microscope, we first imaged a test object that features abrupt spatial changes in the reflectivity. In particular, a 500-nm-thick Ti-coating was sputtered onto a surface of the movable planar sample holder using a patterned metal shield as a mask. In Fig. 3, we show the THz image of the test object $I(x, y)$ [panel (a)], as well as intensity profiles across the lines that contain sharp reflectivity changes [panels (b) and (c)]. The image resolution is then estimated from the full width at half maximum (FWHM) of the spatial derivatives $|dI(x, y')/dx|$ and $|dI(x', y)/dy|$. It is evident from Figs. 3(b) and 3(c) that our THz SI lens provides a deep sub-wavelength-resolution in both OX and OY directions, estimated to be 0.14λ

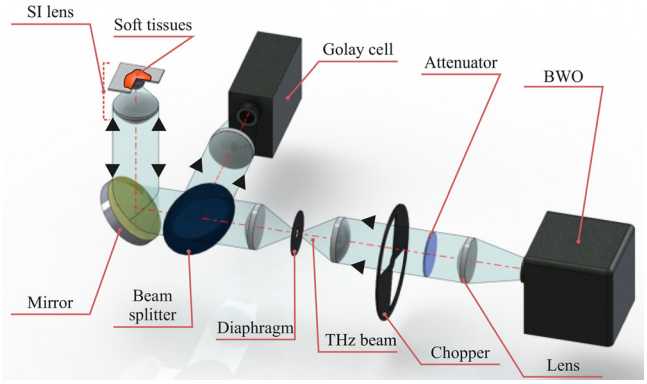

FIG. 2. Schematic of a THz SI microscope for CW reflection-mode imaging of soft tissues.

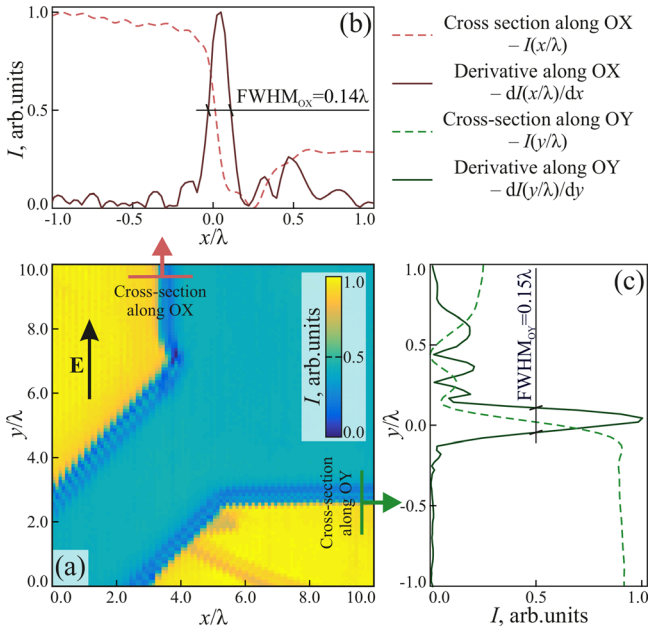

FIG. 3. Experimental estimation of the THz SI microscope resolution at $\lambda = 500\,\mu$m: (a) THz image of a metal test object featuring step-like changes in the refractivity both in OX and OY directions; the vertical black arrow indicates the direction of the electromagnetic wave polarization; (b) and (c) intensity profiles in OX and OY directions, measured near the sharp metal edges of the test object; the first derivatives of these intensity profiles yield estimation of the resolution.

and 0.15λ, correspondingly. Thus, the measured resolution represents a considerable improvement over that of the previously reported configurations of MMW, GHz, and THz SI lenses, namely, 0.3λ,[24] 0.49λ,[25] and 0.35λ.[26] Furthermore, the resolution of our THz SI microscope competes with that of the advanced VIS and IR SI systems, namely, 0.28λ,[22] 0.23λ,[27] 0.2λ,[28] and 0.15–0.31λ.[23]

Such high resolution of our THz SI microscope is achieved thanks to the combined use of a wide aperture aspherical singlet and a high refractive index hemispherical lens. After conducting a comprehensive experimental study, we believe that we have reached the resolution limit of the proposed SI lens configuration with the given materials. Further resolution enhancement can be achieved only by substituting the aspherical singlet with the one featuring a larger NA, or by using the hemisphere material with a higher refractive index than that of a HRFZ-Si. The effective refractive index of the hemisphere might be further increased when using judiciously designed metamaterials[29] or photonic crystals.[30] The depth of field of a SI lens is physically limited by the depth of the evanescent field volume behind the hemisphere. Considering the results of previous theoretical analysis of the hemisphere-based SI lens configurations,[26,31] we expect that the depth of the field is limited to $<\lambda/2$ for the proposed THz SI lens.

Finally, from Fig. 1(b), we notice that both the propagating (transmitted) and evanescent waves contribute to the formation of the THz beam caustic.[32] It is evident that the transverse and longitudinal dimensions of the THz beam caustic depend on the total internal reflection (TIR) conditions at the lens interface and, thus, on the refractive index and microstructure of the object. Such an object-dependent THz beam caustic is an interesting phenomenon, which should be inherent to all configurations of SI optical systems.[31] However, further discussion of this phenomenon is out of the scope of this paper.

In order to highlight potential of THz SI microscopy in biomedicine, we applied our system to imaging of different types of soft tissues. Thus, in Figs. 4(a)–4(c), we demonstrate a photo and THz images of a poinsettia leaf. The THz images correspond to two $8\lambda \times 8\lambda$ square areas of the leaf blade and reveal its sub-wavelength structural elements, such as veins. The intensity of the backscattered THz field is higher for the veins than for the surrounding leaf area, which might be due to differences in the water content, density, and structure of tissues. Next, we applied our setup to imaging of the tissue spheroids made of chondrocytes from the articular hyaline cartilage of male sheep.[33] Each spheroid consists of approximately 8×10^3 chondrocytes and features a diameter of about 300 μm. For the THz imaging, the tissue spheroids were extracted from the growth medium and placed onto the movable planar sample holder. In Figs. 4(d) and 4(e), we show results of THz SI microscopy of a triplet of these spheroids, as well as its optical

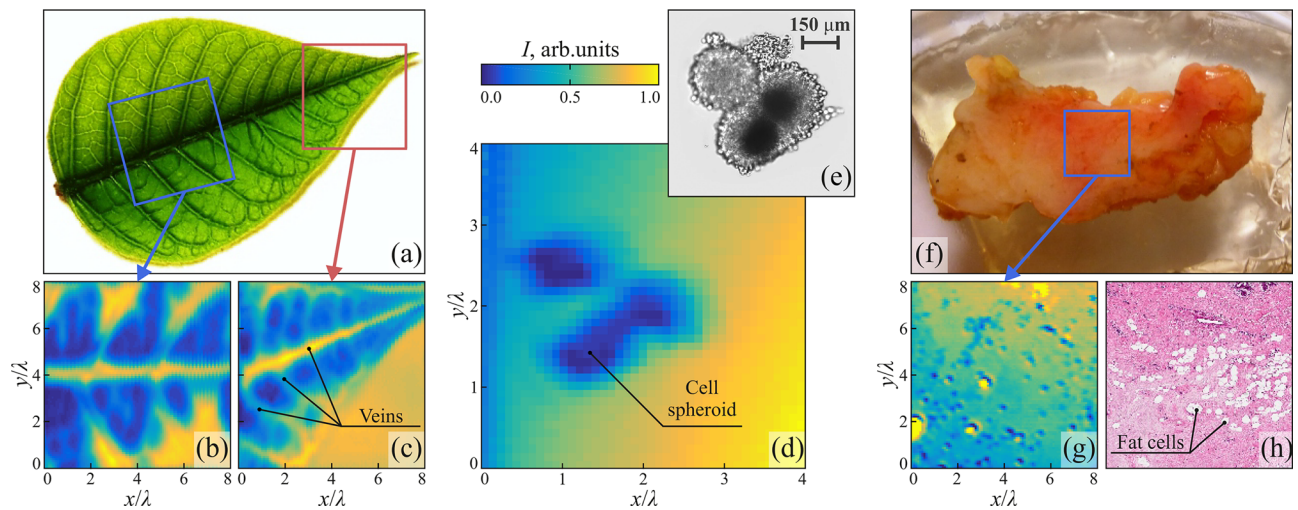

FIG. 4. THz SI microscopy of different soft tissues at $\lambda = 500\,\mu$m: (a)–(c) a photo and THz images of a poinsettia leaf blade; (d) and (e) a THz image and an optical microscopy image of a triplet of the tissue spheroids made of chondrocytes; (f)–(h) a photo, a histology, and a THz image of a human breast specimen *ex vivo* formed by dense fibrous connective tissues, into which single fat cells and their agglomerates are embedded.

microscopy image. Despite the fact that a single spheroid has a sub-wavelength diameter, we could clearly distinguish each spheroid in the THz image of the triplet.

In Figs. 4(f)–4(h), we show the results of the THz SI microscopy of human breast tissue *ex vivo* with fibrocystic mastopathy and foci of adenosis. The breast tissue specimen was excised according to the initial medical diagnosis, and after the THz measurements, the diagnosis was confirmed by histology. In order to prevent the tissue from hydration/dehydration during the THz measurements, we placed them onto the movable planar sample holder and covered with a gelatin film. In panel (h), we observe a fragment of the stroma of the breast *ex vivo*, formed by the dense fibrous connective tissues containing single fat cells and their agglomerates (2–25 cells). Despite the fat cells and their agglomerates being sub-wavelength, they are clearly observed in the THz image. The observed contrast could be due to the lower water content and, thus, lower THz refractive index and absorption coefficient of the fat cells compared to those of the dense fibrous connective tissues.[5] This image highlights the spatially-inhomogeneous character of the breast tissues on the scale set by the THz wavelengths. This could pose limitations to modeling of the THz wave—tissue interactions using a conventional assumption of the homogeneous medium along with relaxation models of the complex dielectric permittivity;[34] hence, the Mie scattering effects should impact the THz response of such tissues. In our opinion, in this case, the radiative transfer theory could form a promising basis for further understanding of THz radiation–tissue interactions.[35]

In this letter, we proposed a method of the THz SI microscopy, which allows imaging of soft tissues with 0.15λ-resolution. We applied it to imaging different types of biological objects. The observed results highlight the prospective of THz SI microscopy in biology and medicine.

This work was supported by the Russian Science Foundation (RSF), Project No. 17-79-20346.

[1]B. Hu and M. Nuss, Opt. Lett. **20**, 1716 (1995).
[2]D. M. Mittleman, S. Hunsche, L. Boivin, and M. C. Nuss, Opt. Lett. **22**, 904 (1997).
[3]X. Yang, X. Zhao, K. Yang, Y. Liu, Y. Liu, W. Fu, and Y. Luo, Trends Biotechnol. **34**, 810 (2016).
[4]V. Wallace, A. Fitzgerald, S. Shankar, N. Flanagan, R. Pye, J. Cluff, and D. Arnone, Br. J. Dermatol. **151**, 424 (2004).
[5]P. Ashworth, E. Pickwell-MacPherson, E. Provenzano, S. Pinder, A. Purushotham, M. Pepper, and V. Wallace, Opt. Express **17**, 12444 (2009).
[6]Y. Ji, S. Oh, S.-G. Kang, J. Heo, S.-H. Kim, Y. Choi, S. Song, H. Son, S. Kim, J. Lee, S. Haam, Y. Huh, J. Chang, C. Joo, and J.-S. Suh, Sci. Rep. **6**, 36040 (2016).
[7]N. Chernomyrdin, M. Frolov, S. Lebedev, I. Reshetov, I. Spektor, V. Tolstoguzov, V. Karasik, A. Khorokhorov, K. Koshelev, A. Schadko, S. Yurchenko, and K. Zaytsev, Rev. Sci. Instrum. **88**, 014703 (2017).
[8]L. Novotny and B. Hecht, *Principles of Nano-Optics*, 2nd ed. (Cambridge University Press, 2012).
[9]Y. Zhang, W. Zhou, X. Wang, Y. Cui, and W. Sun, Strain **44**, 380 (2008).
[10]V. Krozer, T. Loffler, J. Dall, A. Kusk, F. Eichhorn, R. K. Olsson, J. D. Buron, P. U. Jepsen, V. Zhurbenko, and T. Jensen, IEEE Trans. Microwave Theory Tech. **58**, 2027 (2010).
[11]H. Guerboukha, K. Nallappan, and M. Skorobogatiy, Optica **5**, 109 (2018).
[12]H.-T. Chen, R. Kersting, and G. Cho, Appl. Phys. Lett. **83**, 3009 (2003).
[13]A. Huber, F. Keilmann, J. Wittborn, J. Aizpurua, and R. Hillenbrand, Nano Lett. **8**, 3766 (2008).
[14]P. Dean, O. Mitrofanov, J. Keeley, I. Kundu, L. Li, E. Linfield, and A. Giles Davies, Appl. Phys. Lett. **108**, 091113 (2016).
[15]R. Degl'Innocenti, R. Wallis, B. Wei, L. Xiao, S. Kindness, O. Mitrofanov, P. Braeuninger-Weimer, S. Hofmann, H. Beere, and D. Ritchie, ACS Photonics **4**, 2150 (2017).
[16]C. Liewald, S. Mastel, J. Hesler, A. Huber, R. Hillenbrand, and F. Keilmann, Optica **5**, 159 (2018).
[17]B. Lukyanchuk, R. Paniagua-Dominguez, I. Minin, O. Minin, and Z. Wang, Opt. Mater. Express **7**, 1820 (2017).
[18]H. Nguyen Pham, S. Hisatake, O. Minin, T. Nagatsuma, and I. Minin, APL Photonics **2**, 056106 (2017).
[19]L. Yue, B. Yan, J. Monks, R. Dhama, Z. Wang, O. Minin, and I. Minin, J. Infrared, Millimeter, Terahertz Waves **39**, 546 (2018).
[20]S. Mansfield and G. Kino, Appl. Phys. Lett. **57**, 2615 (1990).
[21]G. Lerman, A. Israel, and A. Lewis, Appl. Phys. Lett. **89**, 223122 (2006).
[22]S. Ippolito, S. Thorne, M. Eraslan, B. Goldberg, M. Unlu, and Y. Leblebici, Appl. Phys. Lett. **84**, 4529 (2004).
[23]F. Koklu, J. Quesnel, A. Vamivakas, S. Ippolito, B. Goldberg, and M. Unlu, Opt. Express **16**, 9501 (2008).
[24]A. Pimenov and A. Loidl, Appl. Phys. Lett. **83**, 4122 (2003).
[25]B. Gompf, M. Gerull, T. Muller, and M. Dressel, Infrared Phys. Technol. **49**, 128 (2006).
[26]N. Chernomyrdin, A. Schadko, S. Lebedev, V. Tolstoguzov, V. Kurlov, I. Reshetov, I. Spektor, M. Skorobogatiy, S. Yurchenko, and K. Zaytsev, Appl. Phys. Lett. **110**, 221109 (2017).
[27]D. Fletcher, K. Crozier, C. Quate, G. Kino, K. Goodson, D. Simanovskii, and D. Palanker, Appl. Phys. Lett. **78**, 3589 (2001).
[28]D. Fletcher, K. Crozier, C. Quate, G. Kino, K. Goodson, D. Simanovskii, and D. Palanker, Appl. Phys. Lett. **77**, 2109 (2000).
[29]M. Skorobogatiy, *Nanostructured and Subwavelength Waveguides: Fundamentals and Applications* (Wiley, 2012).
[30]W. Fan, B. Yan, Z. Wang, and L. Wu, Sci. Adv. **2**, e1600901 (2016).
[31]K. Karrai, X. Lorenz, and L. Novotny, Appl. Phys. Lett. **77**, 3459 (2000).
[32]T. Milster, J. Jo, and K. Hirota, Appl. Opt. **38**, 5046 (1999).
[33]E. Koudan, J. Korneva, P. Karalkin, I. Gladkaya, A. Gryadunova, V. Mironov, Y. Khesuani, and E. Bulanova, 3D Print. Addit. Manuf. **4**, 53 (2017).
[34]E. Pickwell, B. Cole, A. Fitzgerald, V. Wallace, and M. Pepper, Appl. Phys. Lett. **84**, 2190 (2004).
[35]V. Tuchin, *Tissue Optics: Light Scattering Methods and Instruments for Medical Diagnostics, Third Edition* (SPIE Press, 2015).